Toxicology 454 (2021) 152743

Contents lists available at ScienceDirect

Toxicology

journal homepage: www.elsevier.com/locate/toxicol

In vitro toxicity of fibrous glaucophane

Alessandro F. Gualtieri [a], Alessandro Zoboli [a], Monica Filaferro [b], Monia Benassi [b], Sonia Scarfì [c], Serena Mirata [c], Rossella Avallone [d], Giovanni Vitale [d], Mark Bailey [e], Martin Harper [f], Dario Di Giuseppe [a,*]

[a] Department of Chemical and Geological Sciences, University of Modena and Reggio Emilia, Modena, Italy
[b] Department of Biomedical, Metabolic and Neurosciences, University of Modena and Reggio Emilia, Modena, Italy
[c] Department of Earth, Environment and Life Sciences, University of Genova, Genova, Italy
[d] Department of Life Sciences, University of Modena and Reggio Emilia, Modena, Italy
[e] Asbestos TEM Laboratories, 600 Bancroft Way, Suite A, Berkeley, CA, USA
[f] Department of Environmental Engineering Sciences, University of Florida, Gainesville, USA

ARTICLE INFO

Keywords:
Fibrous glaucophane
Amphibole asbestos
FPTI
In vitro toxicity
Human lung cells

ABSTRACT

The health hazard represented by the exposure to asbestos may also concern other minerals with asbestos-like crystal habit. One of these potentially hazardous minerals is fibrous glaucophane. Fibrous glaucophane is a major component of blueschist rocks of California (USA) currently mined for construction purposes. Dust generated by the excavation activities might potentially expose workers and the general public. The aim of this study was to determine whether fibrous glaucophane induces *in vitro* toxicity effects on lung cells by assessing the biological responses of cultured human pleural mesothelial cells (Met-5A) and THP-1 derived macrophages exposed for 24 h and 48 h to glaucophane fibres. Crocidolite asbestos was tested for comparison. The experimental configuration of the *in vitro* tests included a cell culture without fibres (*i.e.*, control), cell cultures treated with 50 μg/mL (*i.e.*, 15.6 μg/cm^2) of crocidolite fibres and 25-50–100 μg/mL (*i.e.*, 7.8–15.6–31.2 μg/cm^2) of glaucophane fibres. Results showed that fibrous glaucophane may induce a decrease in cell viability and an increase in extra-cellular lactate dehydrogenase release in the tested cell cultures in a concentration dependent mode. Moreover, it was found that fibrous glaucophane has a potency to cause oxidative stress. The biological reactivity of fibrous glaucophane confirms that it is a toxic agent and, although it apparently induces lower toxic effects compared to crocidolite, exposure to this fibre may be responsible for the development of lung diseases in exposed unprotected workers and population.

1. Introduction

Among the airborne pollutants, asbestos fibres are undoubtedly the most ill-famed ones. The commercial term “asbestos” refers to chrysotile (*i.e.*, the fibrous member of the serpentine group) and five fibrous amphiboles (*i.e.*, amphibole asbestos) that until the ’90s, given their outstanding properties, were mined worldwide and used to manufacture nearly 3000 different composite materials (Gualtieri, 2012). Amphibole asbestos species are actinolite asbestos, amosite (the fibrous variety of cummingtonite-grunerite), anthophyllite asbestos, crocidolite (the fibrous variety of riebeckite), and asbestos tremolite (Alleman and Mossman, 1997; Gualtieri, 2012). Exposure *via* inhalation to asbestos is associated with fatal diseases such as lung cancer, malignant mesothelioma (MM), asbestosis and many others (Kamp, 2009; IARC, 2012, 2017; Carbone et al., 2019). Consequently, the International Agency for Research on Cancer (IARC) included all the six forms of asbestos in *Group 1* “substances carcinogenic to humans” (IARC, 2012).

It is generally recognized that thin and long asbestos fibres, namely those with length >10 μm, width <3 μm and length/width (aspect) ratio >3, can reach the alveolar space and pleural/peritoneal surface, inducing chronic inflammation which prompts adverse effects responsible for the onset of lung cancer and MM (Stanton et al., 1981; Donaldson et al., 2010; Carbone et al., 2019). The cytotoxicity and genotoxicity of asbestos fibres are closely linked to their ability to promote the formation and release of reactive oxygen species (ROS) in the intracellular space (Gualtieri, 2018; Mossman, 2018; Carbone et al., 2019). Long-lasting production of ROS generation (*e.g.*, peroxides, superoxide and hydroxyl radical), overwhelming the antioxidant cell

* Corresponding author at: Department of Chemical and Geological Sciences, University of Modena and Reggio Emilia, Via Campi 103, Modena, 41125, Italy.
E-mail address: ddigiuse@unimore.it (D. Di Giuseppe).

https://doi.org/10.1016/j.tox.2021.152743
Received 13 October 2020; Received in revised form 18 February 2021; Accepted 1 March 2021
Available online 3 March 2021

defence, induces alteration of membrane lipids and proteins, cell injury and DNA damage (Carbone and Yang, 2012; Qi et al., 2013; Wang et al., 2017; Mossman, 2018). The oxidative stress and relative inflammatory process caused by the deposition of asbestos fibres in the lung tissues lead to the growth of cells that have accumulated mutations and are responsible for the pathogenesis and carcinogenesis of asbestos (Carbone et al., 2019). Asbestos fibres trigger the release of ROS either directly, through a surface-mediated mechanism, and indirectly promoting the production of cell-derived radicals (Gualtieri et al., 2019a). In detail, the iron content (essentially Fe^{2+}) at the surface of asbestos fibres, or released by them in the intracellular space, promotes the formation of hydrogen peroxide (H_2O_2) and hydroxyl radicals ($HO^{\bullet}$) *via* the Haber-Weiss cycle [1] and Fenton reaction [2] (Gualtieri et al., 2019a).

$$[1]\ Fe^{2+} + O_2 \rightarrow Fe^{3+} + O_2^{-}$$

$$O_2^{-} + 2H^{+} + e^{-} + H^{+} \rightarrow H_2O_2$$

$$[2]\ Fe^{2+} + H_2O_2 \rightarrow Fe^{+3} + OH^{-} + HO^{\cdot}$$

At the same time, ROS are released during "frustrated" phagocytosis (Donaldson et al., 2010). Frustrated phagocytosis is the failure of alveolar macrophages (mean diameter of ~21 μm; Krombach et al., 1997) to engulf the asbestos fibres (average L > 10 μm; Stanton et al., 1981). During this process, in the attempt to clear the exogenous fibrous particles, macrophages trigger the respiratory burst, *i.e.*, the NADPH oxidase enzyme helps the macrophage to reduce O_2 to a superoxide free radical ($O_2^{\bullet -}$) that rapidly reacts with itself to form H_2O_2 (Babior, 1984; Dahlgren and Karlsson, 1999). $O_2^{\bullet -}$ and H_2O_2 *via* metal-catalysed reaction (see the above-mentioned Fenton reaction [2]) or myeloperoxidase-catalyzed oxidation, generate powerful reactive species such as hydroxyl radicals ($HO^{\bullet}$) and hypochlorite (ClO^{-}) (Babior, 1984; Thomas, 2017).

The pathogenicity and toxicity of asbestos fibres are also related to other structural and physical/chemical characteristics (Gualtieri, 2018) such as morphology (*e.g.*, length and width; Donaldson et al., 2010), chemical composition (*e.g.*, iron and heavy metals content; Gualtieri et al., 2019a, 2019b), surface activity (*e.g.*, zeta potential and cation exchange capacity; Pollastri et al., 2014; Pacella et al., 2017) and biodurability (*i.e.*, the resistance of fibres to chemical/biochemical alteration; Gualtieri et al., 2019b). In nature, a huge number of "unclassified" minerals fibres share the same characteristic of asbestos and therefore their adverse health effects (Adamis et al., 2000; Comba et al., 2003; Carbone et al., 2007; Naik et al., 2017; Zoboli et al., 2019). In particular, the risk posed by unregulated fibrous amphiboles (*e.g.*, winchite and richterite) has been proven by several studies in recent years (Larson et al., 2010; Baumann et al., 2015; Naik et al., 2017), and although they have not yet been classified by the IARC, specific *in vitro* and *in vivo* tests have assessed that they represent a potential hazard for human health (Blake et al., 2007; Baumann et al., 2015; Naik et al., 2017). To date, the only fibrous amphibole, besides the five variety of asbestos, to be classified as carcinogenic by the IARC, is fluoro-edenite (Paoletti et al., 2000; Comba et al., 2003; Cardile et al., 2004). This mineral fibre has been responsible for MM morbidity in some villages in the eastern Sicily (Italy) due to the exposure of the population to fluoro-edenite bearing rocks, extracted from the rocks of the Etna volcanic complex, north-east of Biancavilla, Catania (Gianfagna and Oberti, 2001). The availability of a large dataset from long term epidemiological studies (Paoletti et al., 2000; Fazzo et al., 2012; Comba et al., 2014), *in vivo* carcinogenesis assay and *in vitro* toxicity tests (Travaglione et al., 2003, 2006; Loreto et al., 2008; Musumeci et al., 2010, 2011), lead the IARC to classify fluoro-edenite in the *Group 1* (Grosse et al., 2014; IARC, 2017).

Recently, Erskine and Bailey (2018) pointed out that glaucophane can assume a fibrous habit resembling amphibole asbestos. Glaucophane, from the Greek "glaukos" (bluish-green) and "phanēs" (shining) is an alkaline amphibole whose ideal chemical formula is $Na_2[(Mg,Fe^{2+})_3(Al,Fe^{+3})_2]Si_8O_{22}(OH)_2$. Glaucophane may occur with a fibrous crystal habit in blueschist facies, in former subduction zones or in eclogites that have undergone retrograde metamorphism (Deer et al., 2013). The most notable and extensively blueschist facies terrane in the world is the Franciscan Complex, *i.e.,* a 1000 km long belt of oceanic crust, marine and terrestrial sediments exposed from the California-Oregon border to Los Angeles, USA (Erskine and Bailey, 2018). Fibrous glaucophane is the main mineral component of blueschist rocks of Franciscan Complex (Erskine and Bailey, 2018; Di Giuseppe et al., 2019). As reported by Erskine and Bailey (2018), blueschist rocks from the Franciscan Complex are commonly mined for building/construction purposes in northern and central California (*e.g.*, Calaveras Dam Replacement Project–CDRP) and the dust generated by the excavation activities may potentially expose workers and the nearby populations to adverse health risks. For this reason, fibrous glaucophane may represent a health hazard as naturally occurring asbestos (NOA) and an evaluation of the toxicity and pathogenicity of this mineral fibre is recommended. To this aim, Di Giuseppe et al. (2019) fully characterized a representative sample of fibrous glaucophane from the Franciscan Complex and assessed its toxicity/pathogenicity potential using the fibre potential toxicity index (FPTI) model proposed by Gualtieri (2018). FPTI is a quantitative predictive model of the toxicity/pathogenicity of minerals fibres, based on physical/chemical and morphological parameters (Table 1) that induce biochemical mechanisms responsible for *in vivo* adverse effects (Gualtieri, 2018). This model delivers values of FPTI aimed at ranking the toxicity and pathogenicity of a mineral fibre (Gualtieri, 2018). Although a detailed description of the FPTI parameters is reported in Gualtieri (2018), a short summary is reported in the Supplementary Materials. The results obtained by Di Giuseppe et al. (2019) showed that the FPTI of fibrous glaucophane (FPTI = 2.77) is greater than that of chrysotile asbestos (FPTI = 2.23) and comparable to that of amphibole species like tremolite asbestos (FPTI = 2.88).

The aim of the present study is to assess the *in vitro* cytotoxicity and genotoxicity potential of fibrous glaucophane from the Franciscan Complex. For this purpose, biological responses of human pleural mesothelial Met-5A cells and THP-1 derived macrophages, following exposure to fibrous glaucophane, has been determined by Alamar Blue viability, Extra-cellular LDH and Comet assays. In addition, oxidative stress and ROS generation have been evaluated performing two different

Table 1
Physical/chemical and morphological parameters of the fibre potential toxicity index (FPTI) model to predict *ab initio* the toxicity/pathogenicity of minerals fibres (from Gualtieri, 2018).

Parameter	Matrix element
Morphometric	
length L	(1,1)
diameter D	(1,2)
crystal curvature	(1,3)
crystal habit	(1,4)
fibre density	(1,5)
hydrophobic character of the surface	(1,6)
surface area	(1,7)
Chemical	
total iron content	(1,8)
ferrous iron	(1,9)
surface ferrous iron/iron nuclearity	(1,10)
content of metals other than iron	(1,11)
Biodurability	
dissolution rate	(1,12)
velocity of iron release	(1,13)
velocity of silica dissolution	(1,14)
velocity of release of metals	(1,15)
Surface activity	
zeta potential	(1,16)
fibres' aggregation	(1,17)
cation exchange in zeolites	(1,18)

luminescent assays on Met-5A, THP-1 and A549 cells culture exposed to different concentrations of glaucophane fibres. Crocidolite UICC asbestos standard (South African, NB #4173−111-3) was tested for comparison (Pacella et al., 2019). The outcome of this study is a key step for the regulation of fibrous glaucophane and creates a solid basis for future *in vivo* tests.

2. Material and methods

2.1. Glaucophane fibres

Fibrous glaucophane examined in the present study is from the blueschist metamorphic rocks that belong to the subduction complex Franciscan assemblage in California (late Mesozoic-Tertiary age). Detailed description of Franciscan Complex and occurrence of glaucophane in blueschist rocks was given by Erskine and Bailey (2018). The blueschist rock sample used for our investigations is from the metamorphic rocks outcropping in San Anselmo, Marin County, approximately 15 miles north of San Francisco (USA). Representative samples from this outcrop were collected manually from an easily accessible spot, slightly crushed, quartered and properly homogenized. Bulk rock disaggregation was performed following the protocol suggested by Erskine and Bailey (2018) to obtain a sample representative of the material generated by the crushing and sieving operations realized during the CDRP project. Further information about the sample can be found in the Supplementary Materials. Separation of glaucophane fibres was achieved by hand-picking of the particles, working under a binocular optical microscope. Approximately 50 g of glaucophane fibres was obtained for *in vitro* tests. To verify the success of the separation procedure, the glaucophane-rich sample was examined by Scanning Electron Microscope (SEM) and Transmission Electron Microscope (TEM).

2.2. Electron microscopy

SEM analyses were performed using a FEI Nova NanoSEM 450 FEG-SEM (Hillsboro, OR, USA) with 15 kV accelerating voltage and 3.5 μA beam current and 6 mm working distance.

TEM investigations were conducted using a JEOL F200 instrument (Tokyo, JP), mounting a Cold Field Emission Gun (CFEG) operated at 200 kV. The microscope was equipped with two large area energy-dispersive X-ray spectrometer (EDX) Centurio Silicon Drift Detectors (SDD) (JEOL, Tokyo, JP). Information on crystallinity and *d*-spacing of the crystalline phases can be extracted by taking the Fast Fourier Transform (FFT) of the high-resolution TEM (HRTEM) images. Details on the preparation are provided in the Supplementary Materials.

2.3. Cell cultures used for in vitro tests

Cytotoxicity and genotoxicity effects of the glaucophane fibres were tested using THP-1 (ATCC®, Rockville, MD, USA No. TIB-202) and Met-5A (ATCC®, Rockville, MD, USA No. CRL-9444) cell lines. The THP-1 cell line consists of human leukemia monocytic cells extensively used to study monocyte/macrophage functions (Auwerx, 1991; Gualtieri et al., 2019c). The Met-5A cell line are constituted by human pleural mesothelial cells transformed with SV40 large T antigen from the SV40 virus. This cell line is ideal for detection of potential asbestos and asbestos-like genotoxic effects (Ke et al., 1989; Cardile et al., 2004; Gualtieri et al., 2019c). Cells lines were maintained in controlled atmosphere (37 °C, 5 % CO_2) using RPMI-1640 for THP-1 cells and M-199 for Met-5A cells, supplemented with 10 % fetal bovine serum (Gibco, USA), 100 U/mL penicillin and 100 U/mL streptomycin (Sigma-Aldrich, Milan, Italy). Met-5A also required extra components: 20 mM 4-(2-hydroxyethyl)-1-piperazineethanesulfonic acid (HEPES), 870 nM zinc-free bovine insulin, 400 nM hydrocortisone, 3,3 nM epidermal growth factor (EGF) and Trace-B Elements (finals concentrations are reported on Met-5A guidelines by ATCC). THP-1 required 2 mM L-glutamine (Sigma-Aldrich, Milan, Italy) and phorbol myristate acetate (PMA; 48 nM for 24 h), a tumor-promoting agent to differentiate cells into macrophages before treatments. For cytotoxicity and viability experiments cells were cultured in a 96-well FalconTM plate (70.000 cells/well for THP-1; 15.000 cells/well for Met-5A) while, for genotoxicity test, cells were cultured in a 6-well FalconTM plate (2.000.000 cells/well for THP-1; 650.000 cells/well for Met-5A). All the treatments of the fibres were performed in serum-free conditions using RPMI without phenol red (Corning Fisher Scientific, Milan, Italy).

In addition to Met-5A and THP-1 cells, A549 cell lines were also used to measure intracellular ROS levels. A549 cells were cultured in DMEM (Euroclone ECB75012) supplemented with 10 % FBS (Euroclone ECS0180 L), 2 mM L-Glutamine (Sigma BioXtra G7513), 1x Non-essential amino acids (Sigma M7145), 1 mM Sodium Pyruvate (Sigma S8636), and 1x Antibiotic Antimycotic Solution (AA) (Sigma BioReagent A5955). Cells were cultured at 37 °C, 5% CO_2 humidified air.

2.4. Alamar Blue viability assay

Alamar Blue (AB) is a water-soluble dye used for quantifying *in vitro* viability of various cell lines. When added to cell cultures, the oxidized form of the AB (Cell Viability Reagents Thermo Fisher Scientific Waltham, MA USA) enters the cytosol and is reduced (Al-Nasiry et al., 2007). This redox reaction is accompanied by a shift in colour of the culture medium from indigo blue to pink-violet, which can be easily measured by colorimetric method (absorbance at 570 nm). After a 24 h and 48 h incubation of cell cultures with the mineral fibres (*i.e.*, crocidolite and fibrous glaucophane), 10 μL of AB solution was added. The absorbance was read after additional 2−4 h of incubation using a plate-reading spectrophotometer (Multiskan FC ®Thermo Scientific). The experimental configuration of the AB viability assay included a cell culture without fibres (Ctrl), cell cultures treated with 50 μg/mL (*i.e.*, 15.6 μg/cm^2) of crocidolite fibres and 25-50−100 μg/mL (*i.e.*, 7.8−15.6–31.2 μg/cm^2) concentrations for glaucophane fibres. Treatments were performed in triplicate. This experimental configuration was chosen because it allows a good interaction fibre/cell in culture systems and produces well-defined cellular responses as reported in previous studies (Hamilton et al., 1996; Cardile et al., 2004, 2007a, 2007b; Pugnaloni et al., 2010, 2015; Gualtieri et al., 2019c).

2.5. Extra-cellular LDH assay

Lactate dehydrogenase (LDH) is a cytosol enzyme released by damaged cells into the culture medium. LDH catalysed the oxidation of lactate to pyruvate with reduction of NAD^+ to NADH (Yang et al., 2009). The rate of NAD^+ reduction can be easily measured as an increase in absorbance at 490 nm. LDH assay was performed using the Thermo Scientific Pierce Kit (Pierce Biotechnology Rockford, lL USA) that allows to quantify the released LDH by colorimetric method measurement. After incubation with fibres for 24 and 48 h, an aliquot of 50 μl cell culture medium was transferred into a new plate and mixed with Pierce Kit Reaction Mixture. After a 30 min incubation at room temperature, reactions are interrupted by adding Stop Solution. Absorbance at 490 nm was measured using a plate-reading spectrophotometer to determine LDH activity. The release of LDH from the damaged cells is used as an indicator of cytotoxicity and the level of extracellular LDH is proportional to the number of lysed cells. Cytotoxicity was calculated, dependently on the maximal lysis according to the formula: % cytotoxicity = (experimental value - low control) x 100/ (high control - low control), where low control is assay medium plus cells and high control is assay medium (plus lysis buffer) plus cells. The results were transformed in percentage of controls 100 % in order to have a better comparison among groups. The experimental conditions were the same used for the AB viability assay.

2.6. Alkaline Comet assay

The alkaline Comet assay, also named as Single Cell Gel Electrophoresis (SCGE) assay, is a sensitive method for the detection of DNA damage, widely used to identify substances with genotoxic activity. It was performed using a commercially available kit (OxiSelect™ Comet Assay Kit). Met-5A and THP-1 cells were incubated with crocidolite and glaucophane fibers at a concentration of 50 μg/mL. After 3 h, cells were suspended in molten low-melting-point agarose (OxiSelect™ Comet Agarose 3 - Part No. 235002). Treatments were performed in triplicate. Details on SCGE methods are submitted as Supplementary Materials.

2.7. Reactive oxygen species

Toxicity and carcinogenicity mechanisms of mineral fibres are characterized by a series of processes, among which ROS production is considered the most important (Gualtieri, 2018; Carbone et al., 2019). For this reason, in the present study, the intracellular levels of ROS generated by the exposure to glaucophane fibres were evaluated using two different fluorescent dye-based tests, *i.e.*, 2′,7′-dichloro-dihydro--fluorescein diacetate (DCF) assay and ROS-Glo H_2O_2 assay. Furthermore, in addition to the Met-5A and THP-1 cell lines, the human non-small cell lung carcinoma A549 cell line was tested. A549 cell line was employed in several studies as a cell model for ROS assay (Cardile et al., 2004; Pugnaloni et al., 2015; Wang et al., 2019). As shown by Cardile et al. (2004), A549 cells produce a well-defined cellular response after exposure to fibrous amphiboles (such as crocidolite and fluoro-edenite) and ROS production is dose dependent. These characteristics make A549 cell line very suitable for the study of ROS generated by exposure to fibrous glaucophane.

DCF-based assay is probably the most commonly used test for detecting intracellular ROS and oxidative stress (Aranda et al., 2013; Jovanovic et al., 2019). The cell-permeable DCF diffuses into the cells and in the presence of ROS, rapidly oxidizes to 2′,7′-dichlorofluorescein, which is highly fluorescent and works as a marker for intracellular ROS. DCF tests were performed as already described by Pozzolini et al. (2016) and conducted on Met-5A and THP-1 cell lines. The experimental configuration of the test was as follows: a cell culture without fibres (*i.e.*, control), cell treated with 25.0, 50.0, 75.0 and 100 μg/mL (6.25, 12.5, 18.8, 25.0 μg/cm^2) concentrations of glaucophane fibres. Positive controls were: 100 μg/mL crocidolite and 500 μM H_2O_2.

ROS-Glo H_2O_2 assay (Promega G8820) was used to measure H_2O_2 levels in Met-5A and A549 cell line treated with glaucophane and crocidolite. The experimental configuration of the test was as follows: a cell culture without fibres, cell cultures treated with 12.5, 18.8, 25.0, 37.5, 50.0, 75.0 and 100 μg/mL (3.12, 4.69, 6.25, 9.38, 12.5, 18.8, 25.0 μg/cm^2) concentrations of glaucophane fibres. As positive control of H_2O_2 generation, samples treated with 25 μg/mL (6.25 μg/cm^2) of Croc and menadione at concentration of 8.6 and 17.5 μg/mL, were added to the experiment. Treatments were performed in triplicate.

The ROS-Glo assay is selective for H_2O_2, while the DCF assay is non-discriminatory and is sensitive to different ROS such as $HO^{\bullet}$, $RO_2^{\bullet}$, $RO^{\bullet}$, HOCl, $ONOO^-$and H_2O_2 (Jovanovic et al., 2019). Details of the two ROS test methodology are provided in the Supplementary Materials.

2.8. Statistical analysis

All data were collected in triplicate and expressed as mean ± standard error of means (S.E.M.). Significance was determined by one-way analysis of variance (ANOVA) followed by the Bonferroni post hoc test for multiple comparisons. A p-value of less than 0.05 was considered statistically significant.

3. Results

Representative SEM and TEM images of the glaucophane fibres are reported in Fig. 1 and show that the glaucophane-rich sample used for the *in vitro* tests is characterized by fibres usually arranged in clusters and bundles (Fig. 1a). According to our previous study (see the section 2.1 and the Supplementary Materials), glaucophane single fibres have an average length and width of 4.0 and 0.2 μm, respectively (Fig. 1b). The chemical point analysis of selected fibres (Fig. 1c) shows the characteristic chemical elements of glaucophane from the blueschists of the Franciscan Complex, *i.e.,* Si, Al, Fe, Na and Ca (Lee et al., 1966; Tsujimori et al., 2006; Di Giuseppe et al., 2019). Fig. 1d is an example of FFT pattern extracted from HR-TEM image shown in Fig. 1b. The *d*-spacings (Å) and α angle, determined from the FFT pattern (17.8 Å [010], 5.4 Å [001] and α = 89.91°) match the X-ray diffraction data available from the literature (Di Giuseppe et al., 2019). Cell parameters obtained from FFT coupled with the chemical spot information confirm the purity of the investigated glaucophane sample.

After 24 h exposure to different amounts (25, 50 and 100 μg/mL) of fibrous glaucophane (Gla), viability of THP-1 and Met-5A cells, detected by the Alamar Blue assay, resulted statistically lower than the control (Ctrl) and showed a clear concentration-dependent trend (Fig. 2). The viability of Met-5A treated with 25, 50 and 100 μg/mL of Gla decreased by 10 %, 13 % and 17 %. All the values are lower than those displayed by the Ctrl. Instead, at a concentration of 50 μg/mL, Gla reduces the cell viability of Met-A with lower intensity with respect to Croc (50 μg/mL), although significantly different if compared to Ctrl (Fig. 2a). After 24 h exposure, Alamar Blue viability assay showed that Gla moderately interferes with viability of THP-1 cells at lower concentration (25 μg/mL) with respect to Ctrl, but at 50 or 100 μg/mL it drastically reduces the cell viability. At a concentration of 50 μg/mL, crocidolite was more potent than Gla in reducing the THP-1 cell viability.

LDH levels in THP-1 and Met-5A cultures were in line with the results of the viability assay (Figs. 2 and 3). In fact, compared to Ctrl, LDH levels in cell culture were statistically different and progressively higher as the glaucophane concentration increased (Fig. 3). LDH assay showed that Gla induces no significant cytotoxicity activity in Met-5A cell cultures at the lowest concentration (25 μg/mL). At the same time, the greater concentrations of Gla (50 μg/mL) induce a release of LDH lower to those measured for Croc (50 μg/mL) but significantly higher with respect to Ctrl (Fig. 3a). After 24 h of exposure of Met-5A to Gla (Fig. 3a), the classification of fibres in increasing order of cytotoxicity is: Gla (25 μg/mL) <Gla (50 μg/mL) <Gla (100 μg/mL). Concerning THP-1 cells, treatments with 25 and 50 μg/mL of Gla induce a lower release of LDH compared to Croc (Fig. 3b). At the same incubation time of 24 h, the cytotoxicity of the Gla fibres on the THP-1 cells can be summarized as follows: Gla (25 μg/mL) <Gla (50 μg/mL) <Gla (100 μg/mL).

After 48 h of exposure to Gla, a clear concentration-dependent reduction trend in Met-5A and THP-1 cells viability is observed (Fig. 2). When cells were treated with Gla (25, 50 and 100 μg/mL) and Croc (50 μg/mL) the viability was statistically lower than Ctrl. Viability of Met-5A and THP-1 cells treated with 25 and 50 μg/mL of Gla was statistically higher than that recorded for Croc (50 μg/mL). Met-5A and THP-1 cells viability decreased with increasing incubation time. The decrease is more evident for THP-1 cells than for Met-5A cells (Fig. 2).

Compared to the results obtained after 24 h of exposure, the viability of Met-5A after 48 h of fibres exposure decreased by 5% for the treatment with 50 μg/mL of both Croc and Gla. On the other hand, after exposure to 25 and 100 μg m/L of Gla, the viability of Met-5A decreased by 2 % and 12 %, respectively (Fig. 2a). After 48 h exposure to 25, 50, and 100 μg/mL of Gla, THP-1 viability (compared to 24 h test) decreased by 9, 17, and 21 %, respectively (Fig. 2b). Viability of THP-1 exposed to Croc 50 μg/mL decreased by 13 %. After 48 h of incubation, the viability of THP-1 exposed to 50 μg/mL Gla and 50 μg/mL Croc was significantly lower than the viability of Met-5A exposed to the same concentration of fibres. Instead, low concentration of Gla has little effect on the viability of THP-1 and Met-5A cells (Fig. 2).

After 48 h of Met-5A exposure to Gla and Croc, the LDH release in the medium increased in all treatments with respect to Ctrl (Fig. 3a).

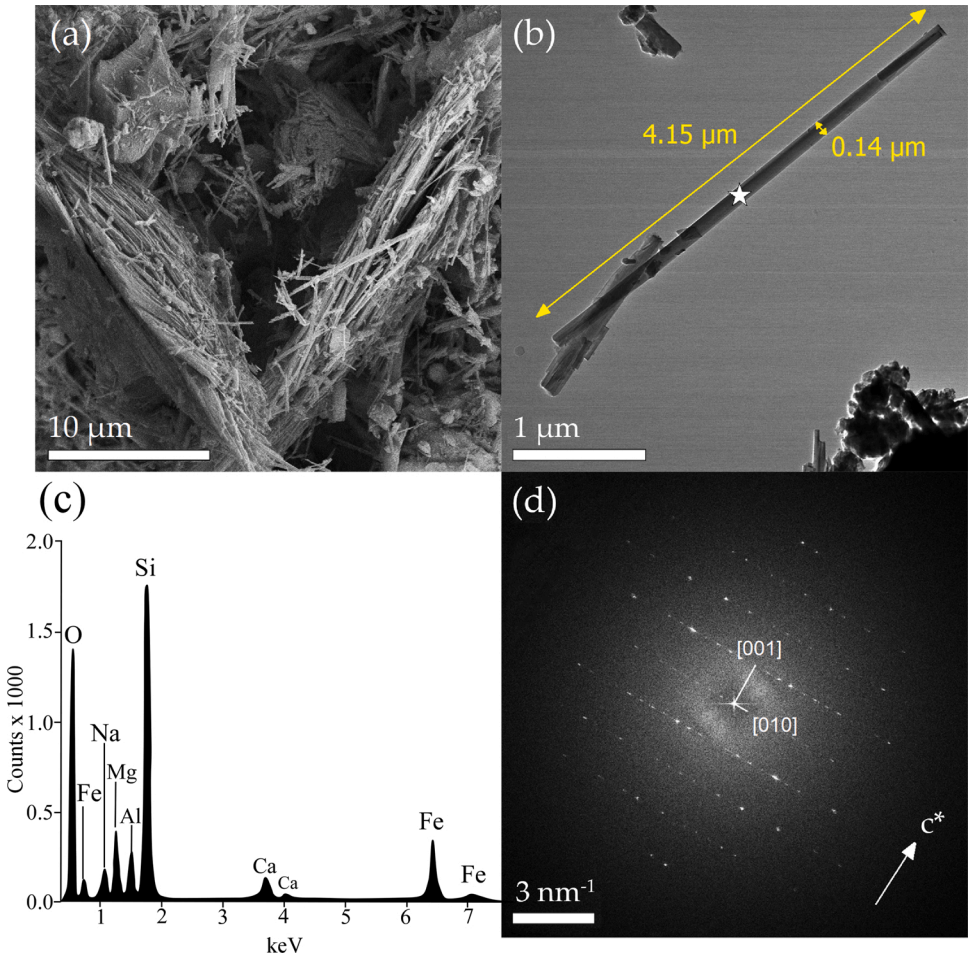

Fig. 1. Electron Microscopy of the glaucophane-rich sample used for the *in vitro* tests. (a) SEM image of the sample. SEM image was acquired using the signal of secondary electrons. Glaucophane fibres are arranged in clusters and bundles. (b) TEM micrograph of an individual glaucophane fibre with average length and width of 4.0 and 0.2 μm, respectively. (c) SEM-EDX spot analysis (white star) of fibre shown in (b). EDX spectra shows the characteristic chemical elements of glaucophane occurred in the blueschist rocks of Franciscan complex, *i.e.,* Si, Al, Na, Fe and Ca. (d) FFT pattern extracted from HRTEM image shown in (b). The cell parameters *d*-spacings (Å) and α angle, determined from the FFT pattern (17.8 Å [010], 5.4 Å [001] and α = 89.91°) match the XRD data available in literature.

Compared to the 24 h test, the LDH release of Met-5A after 48 h exposure to 25, 50 and 100 μg/mL of Gla increased by 20 %, 11 % and 9%, respectively. After 48 h of exposure, Croc induces an increase in LDH release greater than Gla 50 μg/mL. After 48 h of exposure of Met-5A to Gla, the classification of fibres in increasing order of cytotoxicity is: Gla (25 μg/mL) <Gla (50 μg/mL) <Gla (100 μg/mL). LDH release in treated THP-1cells statistically differs from Ctrl after 48 h exposure in Gla at any concentration used, progressively increasing in a concentration dependent fashion (Fig. 3b). The greatest Gla amount (100 μg/mL) induced a 2.6-fold higher release of LDH compared to Ctrl. Croc induced an LDH release (% with respect to Ctrl) of 201 %, whereas concentrations of Gla of 25, 50 and 100 μg/mL induced an LDH release of 136 %, 180 % and 265 %, respectively (Fig. 3b). Compared to the 24 h test, the LDH release of THP-1 after 48 h exposure to 25, 50 and 100 μg/mL of Gla increased by 35 %, 29 % and 58 %, respectively (Fig. 3b). After 48 h of exposure of THP-1 to Gla, the classification of fibres in increasing order of cytotoxicity is: Gla (25 μg/mL) <Gla (50 μg/mL) <Gla (100 μg/mL).

The results of the *in vitro* test show concentration and time dependency for Gla (25, 50 and 100 μg/mL) treatments and the toxicity of this mineral fibre was evidenced by a decrease in cell viability and an increase in LDH release (Figs. 2 and 3). The results show that at the same doses tested, Gla causes less cell viability reduction and less LDH release than Croc.

Results of the alkaline Comet assay obtained exposing Met-5A and THP-1 cells to Croc or Gla (both at concentration of 50 μg/mL) for 3 h, are illustrated in Figs. 4 and 5. Concentration of the fibres and exposure time were optimized on the basis of the results of a series of preliminary tests aimed at reaching cell vitality >80 % before the test, because damaged or dead cells may lead to false positives. Images acquired by epifluorescence microscopy show that the amount of damaged DNA induced by Croc was marked and greater than those induced by Gla (Fig. 4). Met-5A and THP-1 cells treated with Croc and Gla produced several comets with longer and more intense fluorescent tails with respect to Ctrl (Fig. 4). As shown in Fig. 4a and 4d under the electrophoretic conditions, no migration of DNA occurred among the control cells, but clear migration of DNA and extensive cell damage were observed among the cells treated with Croc (Fig. 4b,e) and Gla (Fig. 4 c, f). The parameter considered for the quantitative evaluation of the DNA damage was the tail moment (TM) which proved to be a reliable marker for DNA strand breaks (Fig. 5). For both the cells lines, Gla was able to increase TM with respect to Ctrl but at an intermediate level if compared to Croc (nearly <50 %).

The results of the DCF test for the detection of intracellular ROS production of the THP-1 and Met-5A cell lines exposed to different concentrations of Gla and Croc are shown in Fig. 6. ROS induced by challenging cells with 500 μM H_2O_2 as positive control, is also shown. Since H_2O_2 induced production of intracellular ROS in both cell lines (1.58-fold increase in THP-1 and 1.8 in Met-5A) respect to the negative control, the assay can be considered properly performed. Croc (100 μg/mL) showed a significant induction of ROS production in both cell lines (1.32-fold increase in THP-1 and 1.65 in Met-5A) with respect to the untreated control, showing a higher pro-oxidant effect in Met-5A mesothelial cells (Fig. 6b) with respect to THP-1 macrophages (Fig. 6a). Furthermore, a concentration-dependent induction of ROS in THP-1 and Met-5A cells treated with Gla fibres is observed (Fig. 6). In particular, Gla was able to induce a significant intracellular ROS production after 2 h incubation already at the lowest concentration (25 μg/mL) in both cell lines (1.13-fold increase in THP-1 and 1.32 in Met-5A)

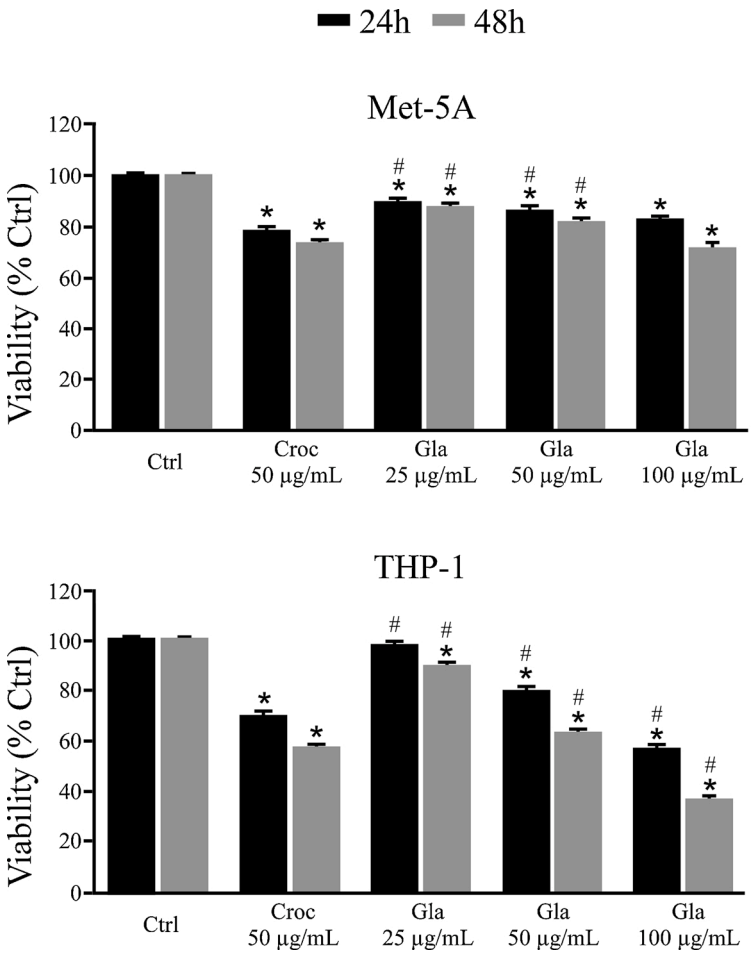

Fig. 2. Results of Alamar Blue viability assay. The graphs show the viability depletion of cultured Met-5A (a) and THP-1 (b) cells treated for 24 and 48 h with 25, 50, 100 µg/mL of Gla or 50 µg/mL of Croc. Cell viability (%) was expressed as a percentage relative to the untreated control cells (Ctrl). Bars represent the standard error of the mean. (*) Values significantly ($p < 0.05$) different with respect to Ctrl, and (#) values significantly different ($p < 0.05$) with respect to Croc. Black and grey bars refer to fibre exposure of 24 h and 48 h, respectively. Gla (fibrous glaucophane); Croc (crocidolite).

with respect to the untreated control. At the highest Gla concentrations, the ROS increase was even more evident (Gla 50 and Gla 100 µg/mL, 1.47 and 1.5-fold increase in THP-1 cells and 1.45 and 1.56 in Met-5A) with respect to the untreated control. Finally, in THP-1 cells, Gla at 50 and 100 µg/mL, showed a ROS production comparable to that of Croc 100 µg/mL, with only Gla 25 showing a significantly lower ROS production compared to Croc ($p < 0.05$). Conversely, in Met-5A the two fibres, Croc and Gla, were comparable only when both were at 100 µg/mL, with the lower concentrations of Gla giving significant lower ROS production with respect to Croc ($p < 0.05$ for both Gla 25 and 50 µg/mL compared to Croc 100 µg/mL).

Fig. 7 shows the H_2O_2 production of the Met-5A and A549 cell lines exposed to different concentrations of Gla and Croc detected with the ROS-Glo assay. Intracellular H_2O_2 production induced by the positive standard menadione is shown in the Supplementary Materials (Fig. S1). Since menadione showed induction of H_2O_2 in all tested cell lines, the assay is considered to be properly performed. Croc at concentration of 25 µg/mL showed a slight, significant, induction of H_2O_2 in all tested cell lines (Fig. 7). Croc displayed the most effective pro-oxidant effect in Met-5A; whereas no difference was found at greater concentrations of Gla (75 and 100 µg/mL) and Croc in terms of H_2O_2 release in A549 cells (Fig. 7). A concentration-dependent induction of H_2O_2 in A549 and Met-5A cells treated with Gla fibres is shown in Fig. 7. The comparison of the luminescence values (RLU) in Gla-exposed and control (Ctrl) cells indicated that Gla displayed a pro-oxidant effect only at greater treatment concentrations (>50 µg/mL). Treatment of cells with 100 µg/mL of Gla induced a 1.4 and 1.5-fold increase in the generation of H_2O_2 compared to Ctrl, in Met-5A and A549 cells, respectively. As shown in Fig. 7, A549 cells were more sensitive to Gla fibres in terms of H_2O_2 generation than Met-5A cells. In fact, the release of H_2O_2 in A549 exposed to Gla (12.5, 18.8, 25.0, 37.5, 50.0, 75.0 and 100 µg/mL) was significantly higher than the H_2O_2 generated in medium of the Met-5A exposed to the same concentrations of fibres (Fig. 7b). In Met-5A cells, a reduction in H_2O_2 release was observed when low concentrations of Gla (≤50 µg/mL) were added to the medium (Fig. 7a).

Hence, it is possible to conclude that Gla stimulates high oxidative stress in THP-1 and A549 cells. Instead, Met-5A cells were found to experience relatively low oxidative stress when exposed to glaucophane fibers. The high oxidative activity of Gla and Croc shown by the DCF test compared to the values shown by the ROS-Glo assay, confirms that these two fibrous amphiboles are capable of generating other ROS in addition to H_2O_2.

4. Discussion

4.1. Toxicity of fibrous glaucophane

Several areas in the USA (*e.g.,* Libby, Montana; Fairfax County, Virginia; El Dorado Hills and Clear Creek, California) are characterized by rocks, sediments and soils containing NOA and represent a potential source of exposure to respirable asbestos fibres for the population (Lee et al., 2008). Noteworthy is the health emergency registered in Libby, Montana, where unclassified fibrous varieties of the amphiboles winchite and richterite contaminated the local vermiculite mine, causing high rates of asbestos-related disease (Carbone et al., 2016). In this framework, the recent guidelines of the Consensus Report of the Weinman International Conference on Mesothelioma suggest to improve characterization of unclassified mineral fibres (size, shape, mineralogy,

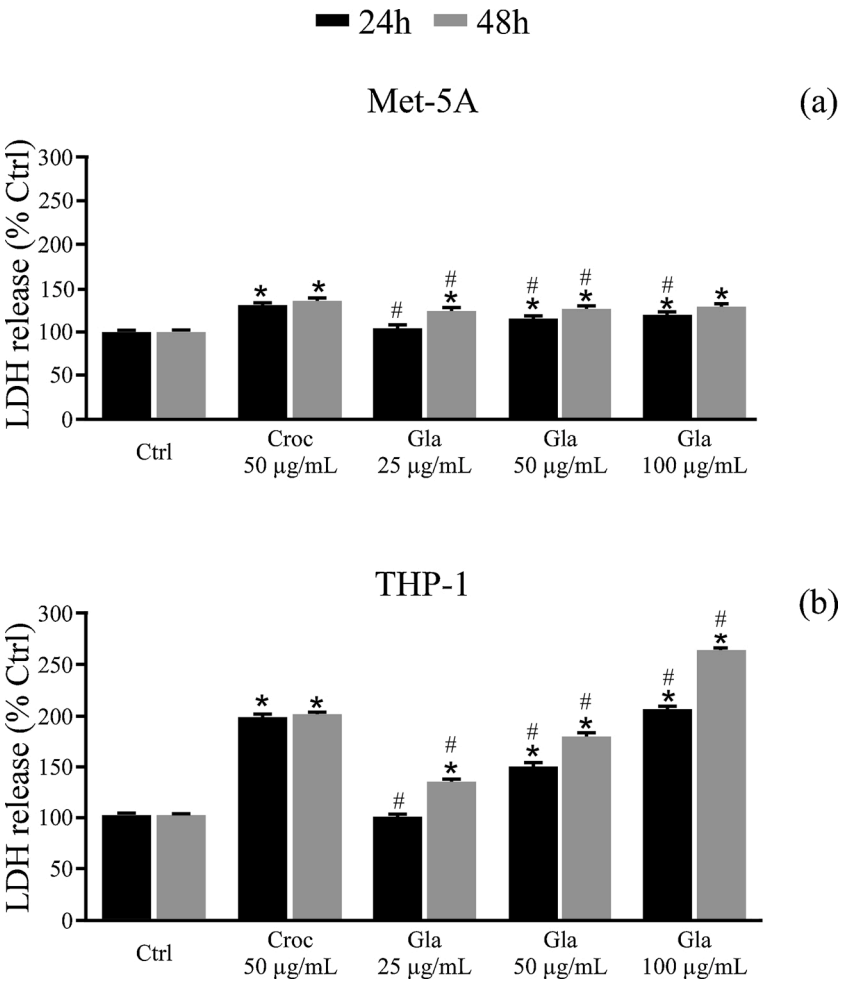

Fig. 3. Lactate dehydrogenase (LDH) (%) released in the medium of Met-5A (a) and THP-1 (b) cells treated with 25, 50, 100 µg/mL of Gla or 50 µg/mL of Croc. The graph shows the effect on LDH released after 24 and 48 h fibres exposure. Released LDH was expressed as a percentage relative to the untreated control cells (Ctrl). Bars represent the standard error of the mean. (*) Values significantly ($p < 0.05$) different with respect to Ctrl, and (#) values significantly different ($p < 0.05$) with respect to Croc. Black and grey bars refer to fibre exposure of 24 h and 48 h, respectively. Gla (fibrous glaucophane); Croc (crocidolite).

surface area, chemistry, *etc.*) and conduct research to better understand their effects on health (Carbone et al., 2016). Because the blueschist of the Franciscan Complex rocks occurs in many localities in California, it is necessary to estimate whether fibrous glaucophane represents a hazard for the general public eventually exposed to this fibrous particulate. To fulfil this gap, in the last three years, an in-depth study has been undertaken to assess the potential toxicity/pathogenicity of fibrous glaucophane (Erskine and Bailey, 2018; Di Giuseppe et al., 2019). Following the FPTI protocol (Gualtieri, 2018; Di Giuseppe et al., 2019), the potential toxicity/pathogenicity of fibrous glaucophane was compared to that of amphibole asbestos species, showing the following rank: amosite (FPTI = 3.17) >asbestos tremolite (FPTI = 2.88) >crocidolite (FPTI = 2.86) >asbestos anthophyllite (FPTI = 2.77) = fibrous glaucophane (FPTI = 2.77) >fibrous fluoro-edenite (FPTI = 2.59). The FPTI of fibrous glaucophane is similar to that of asbestos anthophyllite, but lower than that of amosite, asbestos tremolite and crocidolite. This is explained by the fairly short length of the individual glaucophane fibres (with mean value of 4.0 µm) smaller than the mean values of amphibole asbestos fibres (mean length >20 µm) and below the threshold limit of 8 µm for successful phagocytosis acted by human alveolar macrophages (Stanton et al., 1981). As proposed by different authors (Stanton et al., 1981; Donaldson et al., 2010; Roggli, 2015; Roggli and Green, 2019), fibre length plays a key factor in the pathogenicity of fibres, especially in the development of MM. Long fibres which cannot be successful engulfed by macrophages, lead to frustrated phagocytosis and prompt the release of highly reactive cyto- and genotoxic substances into the extracellular space (Carbone et al., 2019). This model is also supported by the study of Schinwald et al. (2012) indicating that the optimum length of fibre for inducing intrapleural tumours in humans and rats is 5 µm. As far as the morphological parameters are concerned, considerable attention must be paid to the amount and oxidation state of the iron in fibrous glaucophane. Chemical reactivity of fibrous amphiboles (and associated adverse effects) is related to the catalytic activity of iron for the production of ROS, and especially hydroxyl radicals (Gualtieri, 2018). As shown by the data reported in Table 2, only amosite and crocidolite have contents of total iron and ferrous iron higher than fibrous glaucophane. In terms of iron content (and therefore potential chemical reactivity), it is possible to classify fibrous amphibole as follows: amosite > crocidolite > fibrous glaucophane > asbestos anthophyllite > asbestos actinolite > fibrous fluoro-edenite > asbestos tremolite.

Although the FPTI model delivers a quantitative evaluation of the toxicity/pathogenicity of fibrous glaucophane, to assess its actual toxic activity *in vitro*, the chemical-physical-mineralogical information of the fibre must be combined with the biological approach. In the present study, the response of lung cell system to fibrous glaucophane (Gla) exposure was investigated by a set of *in vitro* tests. Data provided by the tests reveal that Gla fibres are able to induce toxic effects in both Met-5A and THP-1 cell lines. According to the Alamar Blue viability assay and the extra-cellular LDH assay, toxic effect of Gla is weak at concentration of 25 µg/mL, moderate at 50 µg/mL and strong or comparable to the positive control Croc (50 µg/mL) at concentrations of 100 µg/mL. Results of *in vitro* studies also highlighted that biological response of Met-5A cells exposed to fibrous glaucophane was remarkably different from that of THP-1. Although glaucophane fibres significantly affect the viability and LDH release of both cell lines, the cytotoxic effect of fibres

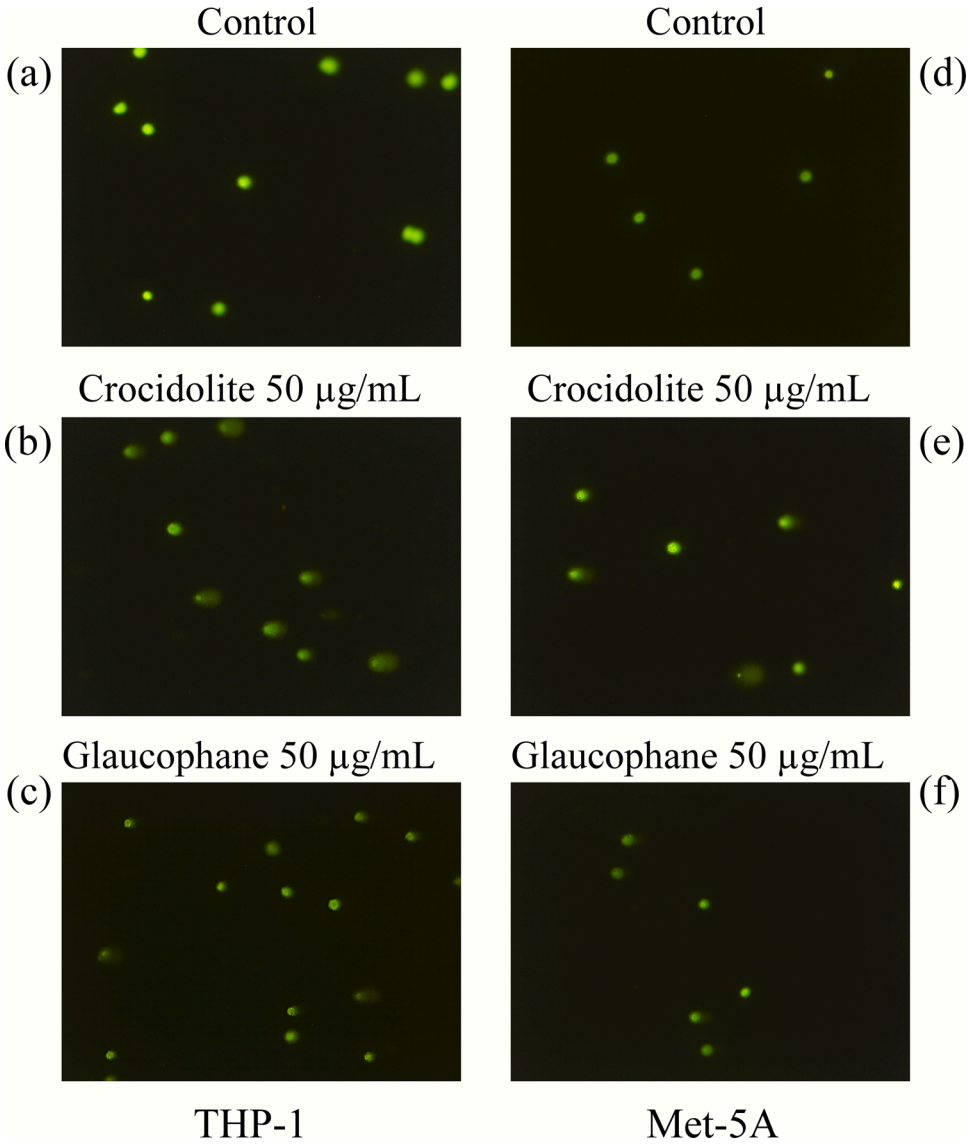

Fig. 4. Comet assay images of THP-1 and Met-5A cells after 3 h of exposure with crocidolite and glaucophane fibres. Large dimensions and high fluorescence of tail are associated with greater DNA damage. (a) Non-exposed THP-1 cells with no induced damage. (b) THP-1 cells exposed to 50 µg/mL of crocidolite fibres. (c) THP-1 cells exposed to 50 µg/mL of glaucophane fibres. (d) Non-exposed Met-5A cells with no induced damage. (e) Met-5A cells exposed to 50 µg/mL of crocidolite fibres. (f) Met-5A cells exposed to 50 µg/mL of glaucophane fibres. Qualitative images of genomic Comet assay show that cells exposed to crocidolite show extensive damage, whereas cells show moderate damage after exposure to glaucophane.

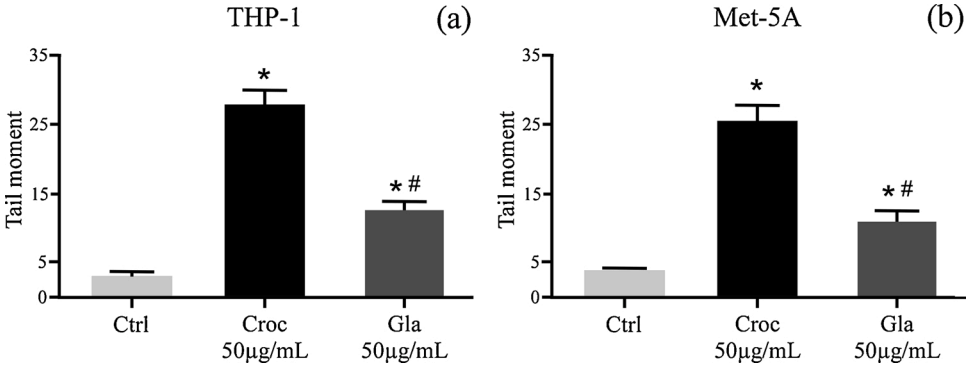

Fig. 5. Effects of a 3 h exposure to 50 µg/mL of Gla and 50 µg/mL of Croc on THP-1 (a) and Met-5A (b) cells evaluated by Alkaline Comet assay tests. The DNA damage is expressed as tail moment (TM) of untreated Met-5A and THP-1cells (Ctrl) and exposed to 50 µg/mL of Croc or Gla for 3 h. (*) Values significantly ($p < 0.05$) different respect to Ctrl, and (#) values significantly ($p < 0.05$) different respect to Croc. Bars represent the standard error of the mean. Gla (fibrous glaucophane); Croc (crocidolite).

was more intense for THP-1 derived macrophages. The vitality of THP-1 after 24 h and 48 h of exposure to 100 µg/mL of glaucophane fibres decreases (with respect to the control) by 40 % and 60 %, respectively. On the other hand, the vitality of Met-5A cells (treated with Gla 100 µg/mL) is reduced only by 30 % after 48 h. In accordance with the viability assay, LDH release was greater for THP-1 cells compared to Met-5A for all the examined fibres (*i.e.*, Croc and Gla). Overall, viability and cytotoxicity induced by Gla in THP-1 derived macrophages after 24 h or 48 h incubation time are inversely correlated and show a clear concentration-dependent profile. The variability of LDH activity and cell viability observed in our study is in line with that observed for other fibrous amphiboles from Libby tested at 20−40 µg/mL on THP-1 cells (Li et al., 2012), fluoro-edenite and crocidolite tested at 5-50−100 µg/mL on mouse monocyte-macrophage J774 and epithelial cancer cell line

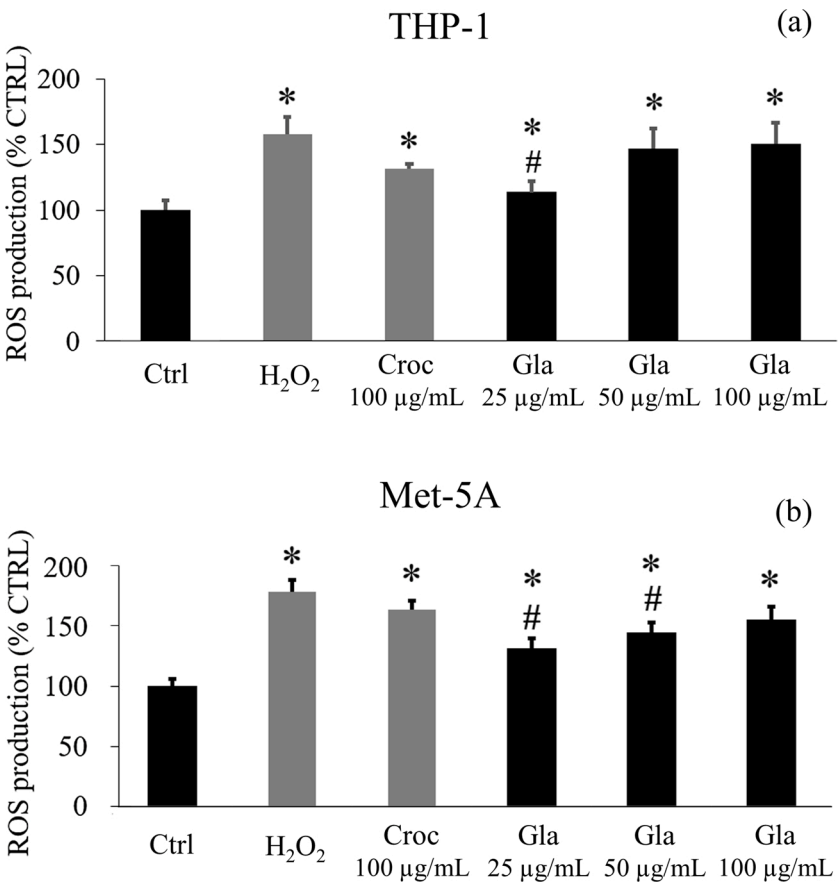

Fig. 6. ROS production (%) by DCF assay in THP-1 (a) and Met-5A (b) cells treated with 25, 50, 100 µg/mL of Gla or 100 µg/mL of Croc. The graph shows the intracellular ROS production measured by the DCF ROS-sensitive dye assay after 2 h fibres exposure. ROS are expressed as a percentage relative to untreated control cells (CTRL). In the same assay, 500 µM H_2O_2 cell exposure for 2 h was used as positive control (H_2O_2 grey bar in both panels). Bars represent the mean ± S.D. of two experiments performed in eightfold for each condition. (*) Values significantly ($p < 0.05$) different with respect to Ctrl, and (#) values significantly different ($p < 0.05$) with respect to Croc. Gla (fibrous glaucophane); Croc (crocidolite).

A549 cells (Cardile, 2004, 2007a, 2007b). Met-5A cell line has been widely employed for *in vitro* cytotoxicity studies of mineral fibres and to a first approximation, the trends shown by previous works employing this cell line are comparable to our results. However, because standard protocols to perform *in vitro* toxicity tests on mineral fibres have not been delivered to date, comparison of the data reported in the literature is difficult. Moreover, it should also be remarked that several parameters can affect result outcomes in particular exposure times. In Cardile et al. (2007a, 2007b) for example, Met-5A cell line was used to study the behaviour of fluoro-edenite (Biancavilla, Italy), fibrous antigorite (Aosta, Italy) and asbestos tremolite (Val di Susa, Italy) with exposure times of 72 h, while in our study the exposure times were 24 h and 48 h.

Our attention is also focused on the presence of genomic DNA breaks in Met-5A and THP-1 derived macrophages exposed to fibrous glaucophane or crocidolite fibres by alkaline Comet assay. According to the obtained results, both types of amphibole fibres induced modifications in comet parameters, as TM increased, demonstrating that DNA damage occurred when cells are exposed to fibrous glaucophane. Genotoxicity of fibrous glaucophane was demonstrated to be significant but less intense than that of Croc. As already highlighted for the Alamar Blue viability and LDH assay tests, the genotoxicity data confirm the predictions of the FPTI model. Comet assay data clearly evidenced the linkage between exposure to the glaucophane fibres and modification of genomic DNA. A possible explanation of the DNA damage induced by the Gla fibres is their ability to prompt the generation of oxidative metabolites like H_2O_2. Literature data (Xu et al., 2002; Cardile et al., 2004; 2007a; 2007b; Helmig et al., 2018) support this observation as amphibole fibres induced oxidative stress, whose critical role in the cell injury is well known. Our results on the ROS detection assays confirm that Gla and Croc fibres are capable to initiate an oxidative process in all the tested cell lines (Figs. 6 and 7). However, tests conducted on Met-5A and A549 cells show that Gla induces a lower release of H_2O_2 than Croc (Fig. 7). Oxidative burst elicited by Gla is limited by its chemical-physical properties. Gla has a lower Fe content, therefore, H_2O_2 production through the Haber-Weiss cycle is obviously lower than that generated by iron-rich asbestos such as amosite and Croc (Table 2).

It should be remarked that low concentrations of ROS cause cell proliferation, while high concentrations of ROS induce apoptosis or necrosis (Day and Suzuki, 2005; Schieber and Chandel, 2014). Since we observed that Gla fibres at the highest concentrations elicit a significant oxidative burst, which is comparable to that of Croc fibres in both cell lines (Figs. 6 and 7), we could infer that both types of fibres are likely able to induce cell damage, at least when administered at high concentration. This model applies to THP-1 macrophages, where the cytotoxicity tests (Figs. 2 and 3) clearly demonstrate very high and comparable cell death rates in Gla treated cells (50 and 100 µg/mL) with respect to Croc (50 µg/mL). In Met-5A cells, we also observe comparable cell death rates between Gla at 100 µg/mL and Croc at 50 µg/mL but different trends with respect to THP-1 cells (Fig. 2). Although ROS production is significant in both cell lines when they interact with the Gla fibres (Fig. 6), Met-5A cell rate survival in presence of the fibres (both Gla and Croc) is significantly higher, with these cells only slightly affected if compared to THP-1 macrophages (Fig. 2). This anomaly is likely explained by the anti-oxidant compensating mechanisms of Met-5A lung cells, which enable these cells to cope with the initial increase of ROS production upon Gla and Croc stimulation, counterbalancing the increase of ROS levels by the activity of anti-oxidant proteins able to protect from cell damage (Kinnula et al., 1994; Schieber and Chandel, 2014). It should also be noted that, in relation to THP-1 macrophages, Met-5A cells are not efficient phagocytes so the increased toxicity of Gla observed in THP-1 cells can be attributed to phagocytosis which does not significantly occur in Met-5A.

Phagocytosis, a bio-chemical process influenced by the size of the target fibre, may also explain why the ROS production induced by Gla 50

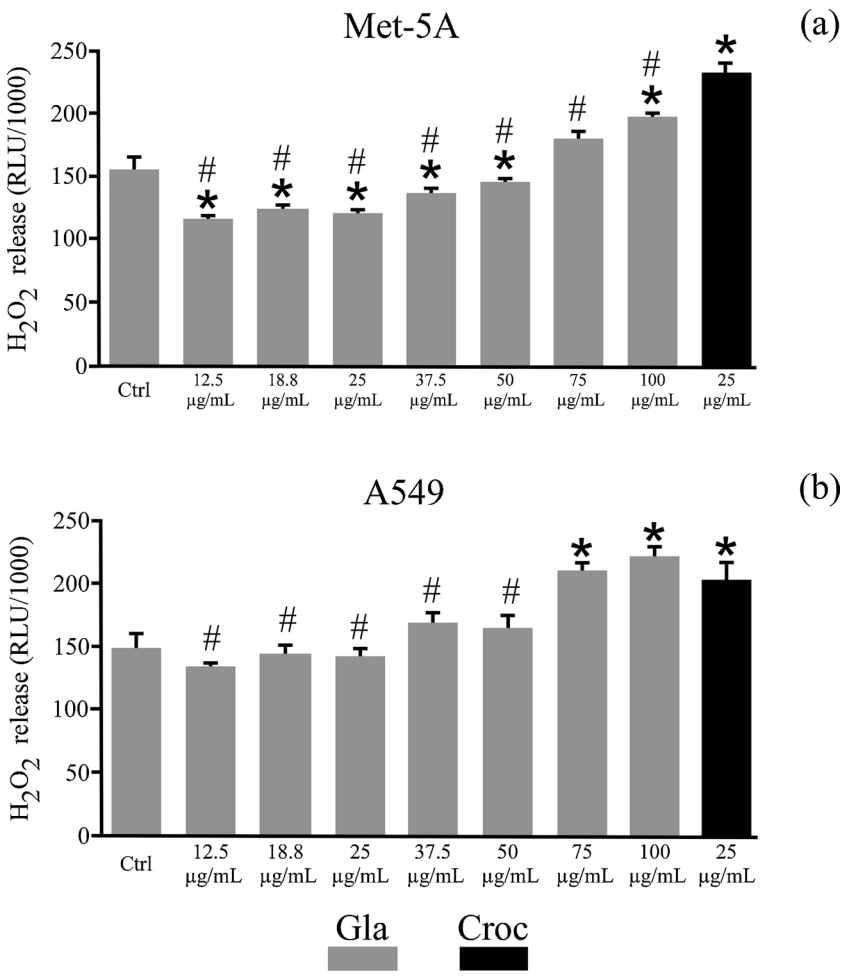

Fig. 7. Concentration response of H_2O_2 relished by (a) Met-5A, (b) A549 cell lines in response to various concentration of Gla (grey bars). Exposure time is 2.5 h. Croc at concertation of 25 µg/mL was also tested for comparison (black bar). Data were obtained by ROS-Glo H_2O_2 assay and expressed in Relative Luminescence Unit (RLU). RLU values are proportional to H_2O_2 levels in cells treated with tested fibres at indicated concentrations. (*) Values significantly ($p < 0.05$) different respect to Ctrl, and (#) values significantly ($p < 0.05$) different respect to Croc. Bars represent the standard error of the mean. Gla (fibrous glaucophane); Croc (crocidolite).

Table 2
Mean ferrous and ferric iron content in fibrous glaucophane, fluoro-edenite and amphibole asbestos. Data are reported as oxide weight percentages.

Mineral fibre	Fe_2O_3	FeO	Sum	Reference
amosite	4.0	38	42	Pollastri et al. (2017a)
crocidolite	18	17	35	Pacella et al. (2019)
glaucophane	6.0	11	17	Di Giuseppe et al. (2019)
anthophyllite	0.0	10	10	Pollastri et al. (2017a)
actinolite	1.0	7.0	8.0	Pollastri et al. (2017b)
fluoro-edenite	1.0	1.6	2.6	Gianfagna and Oberti (2001)
tremolite	0.2	1.0	1.2	Ballirano et al. (2008)

and 100 µg/mL is comparable to the ROS production induced by Croc 100 µg/mL (Fig. 6a). THP-1 are active phagocytic cells, accumulate a cellular dose through dynamic movement and tend to engulf all the fibres they are exposed to. It is possible to speculate that, in closed systems such as that of *in vitro* tests, the probability that THP-1 macrophages engulf short Gla fibres (mean L = 4.0 µm) is much higher than the probability they engulf long Croc fibres (mean L > 10 µm). Therefore, with respect to long Croc fibres, a higher number of phagocytosis events of short Gla fibres by THP-1 cells prompt a higher oxidative stress.

4.2. Implications for the excavation activities in California

The result of this study is the first step forward to understanding the actual toxicity/pathogenicity of fibrous glaucophane. As stated in the Introduction, fibrous blueschist deposits within the Franciscan Complex have been recently excavated in California for the Calaveras Dam Replacement Project (CDRP). Without recognition of fibrous glaucophane as a hazard, the employer could reasonably consider themselves exempt from local, State, and Federal regulations. However, a concern was raised that the dust generated by the excavation activities might potentially expose workers and the general public to adverse health risks. For this reason, the owner of the dam, the San Francisco Public Utilities Commission, employed the precautionary principle and assumed that fibrous glaucophane represents a potential health hazard as NOA, although an evaluation of the potential health hazard of this mineral fibre had not been undertaken before the publication of this work. Air monitoring data from CDRP document the high potential of air exposures to the public and site workers from blueschist rock dust, *i.e.*, a mixture of amphiboles in glaucophane is the dominant species (Erskine and Bailey, 2018). During periods of intense blueschist disturbance activities, the concentrations of the glaucophane fibres usually exceed perimeter thresholds (based on asbestos risk), and exposures to certain workers may overcome the US federal asbestos permissible exposure limit (PEL). It should be remarked that glaucophane is not a regulated amphibole in California or the US so there is no PEL for exposure to it. The National Institute for Occupational Safety and Health (NIOSH) does consider any amphibole in the glaucophane-riebeckite solid solution to be considered hazardous, but the strict regulations do not include glaucophane (NIOSH, 1994a, b). Although the blueschist rocks of the Franciscan Complex are composed predominantly of short fibres (about 7% of the fibres of the CDRP bulk samples are long), it is the number of long fibres in fugitive emissions rather than the percent present in rock and soil that is important.

The potential of adverse exposures to fibrous glaucophane in northern California, as well as other locations where Franciscan rocks

are disturbed, is significant and previously unrecognized. For example, the City and County of San Francisco and majority of the Silicon Valley and surrounding areas to the south are underlain by the Franciscan Complex or Franciscan-derived alluvium. These are areas of intense development, and large construction projects involving commercial buildings and residential subdivisions in close proximity to existing populations are a ubiquitous presence.

5. Conclusions

The prediction of the FPTI model that fibrous glaucophane from Franciscan Complex, California, is a potential toxic/pathogenic mineral fibre is confirmed by the results of this *in vitro* toxicity study. In particular, the results of *in vitro* tests confirm that fibrous glaucophane has the potential to induce cell death, DNA damage and oxidative stress, Overall, the rank of the investigated fibres in increasing order of cytotoxicity is: Gla (25 μg/mL) <Gla (50 μg/mL) <Gla (100 μg/mL). As noted by Erskine and Bailey (2018) fibrous glaucophane is likely to be respirable when dust from blueschist rocks is released into the environment. Although fibrous glaucophane apparently induces lower toxic effects compared to carcinogenic crocidolite, the inhalation of glaucophane fibres may be hypothetically responsible for the development of lung diseases. For a conclusive understanding of the mechanisms of the cellular/tissues responses to fibrous glaucophane, *in vivo* animal tests should be performed and compared to the outcome of the *in vitro* tests.

Because the occurrence of fibrous glaucophane concerns widespread geologic formations (*i.e.*, Franciscan Complex) this mineral fibre should be considered a health hazard and the precautionary approach applied during the excavation activities concerning the blueschist rocks. A preventive action is hence justified to avoid the situations similar to the fluoro-edenite Biancavilla case and the NOA-related issues in Libby.

CRediT authorship contribution statement

Alessandro F. Gualtieri: Conceptualization, Funding acquisition, Writing - review & editing. **Alessandro Zoboli:** Formal analysis, Writing - review & editing. **Monica Filaferro:** Formal analysis, Writing - review & editing. **Monia Benassi:** Formal analysis, Writing - review & editing. **Sonia Scarfì:** Formal analysis, Writing - review & editing. **Serena Mirata:** Formal analysis, Writing - review & editing. **Rossella Avallone:** Supervision, Validation, Writing - review & editing. **Giovanni Vitale:** Supervision, Validation, Writing - review & editing. **Mark Bailey:** Supervision, Validation, Writing - review & editing. **Martin Harper:** Supervision, Validation, Writing - review & editing. **Dario Di Giuseppe:** Formal analysis, Writing - review & editing.

Declaration of Competing Interest

The authors report no declarations of interest.

Acknowledgements

This research was conducted earlier under the Fondi di Ateneo per la Ricerca (FAR 2017) "Fibre potential toxicity Index (FPTI). A quantitative model to evaluate the toxicity and pathogenicity of mineral fibres, including asbestos" and later under the project "*Fibres A Multidisciplinary Mineralogical, Crystal-Chemical and Biological Project to Amend the Paradigm of Toxicity and Cancerogenicity of Mineral Fibres*" (PRIN – Bando 2017 - Prot. 20173 × 8WA4). The TEM image and related EDS spectrum were collected during the stay of A.Z. at the Department of Earth and Environmental Science, University of Pennsylvania, under the supervision of Dr. Ruggero Vigliaturo who is kindly acknowledged for his support. Thanks are due to Kitos Biotech lab for the H_2O_2 assay. Two anonymous referees are kindly acknowledged for their useful comments and suggestions which greatly improved the quality of the final version of the manuscript.

Appendix A. Supplementary data

Supplementary material related to this article can be found, in the online version, at doi:https://doi.org/10.1016/j.tox.2021.152743.

References

Adamis, Z., Tatrai, E., Honma, K., Six, E., Ungvary, G., 2000. *In vitro* and *in vivo* tests for determination of the pathogenicity of quartz, diatomaceous earth, mordenite and clinoptilolite. Ann. Occup. Hyg. 44, 67–74.
Alleman, J.E., Mossman, B.T., 1997. Asbestos revisited. Sci. Am. 277, 54–57.
Al-Nasiry, S., Geusens, N., Hanssens, M., Luyten, C., Pijnenborg, R., 2007. The use of Alamar Blue assay for quantitative analysis of viability, migration and invasion of choriocarcinoma cells. Hum. Rep. 22, 1304–1309.
Aranda, A., Sequedo, L., Tolosa, L., Quintas, G., Burello, E., Castell, J.V., Gombau, L., 2013. Dichloro-dihydro-fluorescein diacetate (DCFH-DA) assay: a quantitative method for oxidative stress assessment of nanoparticle-treated cells. Toxicol. In Vitro 27, 954–963.
Auwerx, J., 1991. The human leukemia cell line, THP-1: a multifacetted model for the study of monocyte-macrophage differentiation. Experientia 47, 22–31.
Babior, B.M., 1984. The respiratory burst of phagocytes. J. Clin. Invest. 73, 599–601.
Ballirano, P., Andreozzi, G.B., Belardi, G., 2008. Crystal chemical and structural characterization of fibrous tremolite from Susa Valley, Italy, with comments on potential harmful effects on human health. Am. Mineral. 93, 1349–1355.
Baumann, F., Buck, B.J., Metcalf, R.V., McLaurin, B.T., Merkler, D.J., Carbone, M., 2015. The presence of asbestos in the natural environment is likely related to mesothelioma in young individuals and women from Southern Nevada. J. Thorac. Oncol. 10, 731–737.
Blake, D.J., Bolin, C.M., Cox, D.P., Cardozo-Pelaez, F., Pfau, J.C., 2007. Internalization of Libby amphibole asbestos and induction of oxidative stress in murine macrophages. Toxicol. Sci. 99, 277–288.
Carbone, M., Yang, H., 2012. Molecular pathways: targeting mechanisms of asbestos and erionite carcinogenesis in mesothelioma. Clin. Cancer Res. 18, 598–604.
Carbone, M., Emri, S., Dogan, A.U., Steele, I., Tuncer, M., Pass, H.I., Baris, Y.I., 2007. A mesothelioma epidemic in Cappadocia: scientific developments and unexpected social outcomes. Nat. Rev. Cancer 7, 147–154.
Carbone, M., Kanodia, S., Chao, A., Miller, A., Wali, A., Weissman, D., Adjei, A., Baumann, F., Boffetta, P., Buck, B., de Perrot, M., Dogan, A.U., Gavett, S., Gualtieri, A., Hassan, R., Hesdorffer, M., Hirsch, F.R., Larson, D., Mao, W., Masten, S., Pass, H.I., Peto, J., Pira, E., Steele, I., Tsao, A., Woodard, G.A., Yang, H., Malik, S., 2016. Consensus report of the 2015 Weinman International Conference on mesothelioma. J. Thorac. Oncol. 11 (8), 1246–1262.
Carbone, M., Adusumilli, P.S., Alexander Jr., H.R., Baas, P., Bardelli, F., Bononi, A., Bueno, R., Felley-Bosco, E., Galateu-Salle, F., Jablons, D., Mansfield, A.S., Minaai, M., de Perrot, M., Pesavento, P., Rusch, v., Severon, D.T., Taioli, e., Tsao, A., Woodard, G., Yang, H., Zauderer, G., Pass, H.I., 2019. Mesothelioma: scientific clues for prevention, diagnosis, and therapy. CA-Cancer J. Clin. 69, 402–429.
Cardile, V., Renis, M., Scifo, C., Lombardo, L., Gulino, R., Mancari, B., Panico, A., 2004. Behaviour of the new asbestos amphibole fluoro-edenite in different lung cell systems. Int. J. Biochem. Cell Biol. 36, 849–860.
Cardile, V., Lombardo, L., Belluso, E., Panico, A., Capella, S., Balazy, M., 2007a. Toxicity and carcinogenicity mechanisms of fibrous antigorite. Int. J. Environ. Res. Public Health 4, 1–9.
Cardile, V., Lombardo, L., Belluso, E., Panico, A., Renis, M., Capella, S., Balazy, M., 2007b. Fluoro-edenite fibers induce expression of Hsp70 and inflammatory response. Int. J. Environ. Res. Public Health 4, 195–202.
Comba, P., Gianfagna, A., Paoletti, L., 2003. Pleuralmesotheliomacases in Biancavilla are related to a new fluoro-edenite fibrousamphibole. Arch. Environ. Health 58, 229–232.
Comba, P., Ricci, P., Iavarone, I., Pirastu, R., Buzzoni, C., Fusco, M., Ferretti, S., Fazzo, L., Pesetto, R., Zona, A., Crocetti, E., 2014. Cancer incidence in Italian contaminated sites. Ann. Ist. Super. Sanità. 50, 2.
Dahlgren, C., Karlsson, A., 1999. Respiratory burst in human neutrophils. J. Immunol. Methods 232, 3–14.
Day, R.M., Suzuki, Y.J., 2005. Cell proliferation, reactive oxygen and cellular glutathione. Dose-Response 3, 425–442.
Deer, W.A., Howie, R.A., Zussman, J., 2013. An Introduction to the Rock-Forming Minerals, third ed. Mineralogical Society of Great Britain and Ireland, London.
Di Giuseppe, D., Harper, M., Bailey, M., Erskine, B., Della Ventura, G., Ardith, M., Pasquali, L., Tomaino, G., Ray, R., Mason, H., Dyar, M.D., Hanuskova, M., Giacobbe, C., Zoboli, A., Gualtieri, A.F., 2019. Characterization and assessment of the potential toxicity/pathogenicity of fibrous glaucophane. Environ. Res. 178, 108723.
Donaldson, K., Murphy, F.A., Duffin, R., Poland, C.A., 2010. Asbestos, carbon nanotubes and the pleural mesothelium: a review of the hypothesis regarding the role of long fibre retention in the parietal pleura, inflammation and mesothelioma. Part. Fibre Toxicol. 7, 5.
Erskine, B.G., Bailey, M., 2018. Characterization of asbestiform glaucophane-winchite in the Franciscan Complex blueschist, northern Diablo Range, California. Toxicol. Appl. Pharm. 361, 3–13.
Fazzo, L., De Santis, M., Minelli, G., Bruno, C., Zona, A., Marinaccio, A., Conti, S., Comba, P., 2012. Pleural mesothelioma mortality and asbestos exposure mapping in Italy. Am. J. Ind. Med. 55, 11–24.

Gianfagna, A., Oberti, R., 2001. Fluoro-edenite from Biancavilla (Catania, Sicily, Italy): crystal chemistry of a new amphibole end-member. Am. Mineral. 86, 1489–1493.
Grosse, Y., Loomis, D., Guyton, K.Z., Lauby-Secretan, B., El Ghissassi, F., Bouvard, V., Benbrahim-Tallaa, L., Guha, N., Scoccianti, C., Mattock, H., Straif, K., 2014. Carcinogenicity of fluoro-edenite, silicon carbide fibres and whiskers, and carbon nanotubes. Lancet Oncol. 15, 1427–1428.
Gualtieri, A.F., 2012. Mineral fibre-based building materials and their health hazards. In: Pacheco-Torgal, F., Jalali, S., Fucic, A. (Eds.), Toxicity of Building Materials. Woodhead, Cambridge, pp. 166–195.
Gualtieri, A.F., 2018. Towards a quantitative model to predict the toxicity/pathogenicity potential of mineral fibers. Toxicol. Appl. Pharm. 361, 89–98.
Gualtieri, A.F., Andreozzi, G.B., Tomatis, M., Turci, F., 2019a. Iron from a geochemical viewpoint. Understanding toxicity/pathogenicity mechanisms in iron-bearing minerals with a special attention to mineral fibers. Free Radical. Bio. Med. 133, 21–37.
Gualtieri, A.F., Lusvardi, G., Zoboli, A., Di Giuseppe, D., Lassinantti Gualtieri, M., 2019b. Biodurability and release of metals during the dissolution of chrysotile, crocidolite and fibrous erionite. Environ. Res. 171, 550–557.
Gualtieri, A.F., Lusvardi, G., Pedone, A., Di Giuseppe, D., Zoboli, A., Mucci, A., Zambon, A., Filaferro, M., Vitale, G., Benassi, M., Avallone, R., Pasquali, L., Lassinantti Gualtieri, M., 2019c. Structure model and toxicity of the product of biodissolution of chrysotile asbestos in the lungs. Chem. Res. Toxicol. 32, 2063–2077.
Hamilton, R.F., Iyer, L.L., Holian, A., 1996. Asbestos induces apoptosis in human alveolar macrophages. Am. J. Physiol-Lung C. 271, 813–819.
Helmig, S., Walter, D., Putzier, J., Maxeiner, H., Wenzel, S., Schneider, J., 2018. Oxidative and cytotoxic stress induced by inorganic granular and fibrous particles. Mol. Med. Rep. 17, 8518–8529.
IARC, 2012. Arsenic, Metals, Fibres and Dust. IARC Monographs on the Evaluation of Carcinogenic Risks to Humans Volume 100c. International Agency for Research on Cancer, Lyon.
IARC, 2017. Some Nanomaterials and Some Fibres. IARC Monographs on the Evaluation of Carcinogenic Risks to Humans, Vol. 111. International Agency for Research on Cancer, Lyon.
Jovanovic, M.V., Savic, J.Z., Salimi, F., Stevanovic, S., Brown, R.A., Jovasevic-Stojanovic, M., Manojlovic, D., Bartonova, A., Bottle, S., Ristovski, Z.D., 2019. Measurements of oxidative potential of particulate matter at Belgrade tunnel; comparison of BPEAnit, DTT and DCFH assays. Int. J. Environ. Res. 16, 4906.
Kamp, D.W., 2009. Asbestos-induced lung diseases: an update. Transl. Res. 153, 143–152.
Ke, Y., Reddel, R.R., Gerwin, B.I., Reddel, H.K., Somers, A.N.A., Mc Menamin, M.G., La Veck, M.A., Stahel, R.A., Lechner, J., Harris, C.C., 1989. Establishment of a human in vitro mesothelial cell model system for investigating mechanisms of asbestos-induced mesothelioma. Am. J. Pathol. 134, 979–991.
Kinnula, V.L., Aalto, K., Raivio, K.O., Walles, S., Linnainmaa, K., 1994. Cytotoxicity of oxidants and asbestos fibers in cultured human mesothelial cells. Free Radical Bio. Med. 16, 169–176.
Krombach, F., Münzing, S., Allmeling, A.M., Gerlach, J.T., Behr, J., Dörger, M., 1997. Cell size of alveolar macrophages: an interspecies comparison. Environ. Heal. Perspect. 105, 1261–1263.
Larson, T.C., Antao, V.C., Bove, F.J., 2010. Vermiculite worker mortality: estimated effects of occupational exposure to Libby amphibole. J. Occup. Environ. Med. 52, 555–560.
Lee, D.E., Coleman, R.G., Bastron, H., Smith, V.C., 1966. A Two-amphibole Glaucophane Schist in the Franciscan Formation, Cazadero Area, Sonoma County. US Geol Surv, Prof Pap, California, pp. C148–C157.
Lee, R.J., Strohmeier, B.R., Bunker, K.L., Van Orden, D.R., 2008. Naturally occurring asbestos—a recurring public policy challenge. J. Hazard. Mater. 153, 1–21.
Li, M., Gunter, M.E., Fukagawa, N.K., 2012. Differential activation of the inflammasome in THP-1 cells exposed to chrysotile asbestos and Libby "six-mix" amphiboles and subsequent activation of BEAS-2B cells. Cytokine 60, 718–730.
Loreto, C., Rapisarda, V., Carnazza, M.L., Musumeci, G., Valentino, M., Fenga, C., Martinez, G., 2008. Fluoro-edenite fibres induce lung cell apoptosis: an *in vivo* study. Histol. Histopathol. 23, 319–326.
Mossman, B.T., 2018. Mechanistic *in vitro* studies: what they have told us about carcinogenic properties of elongated mineral particles (EMPs). Toxicol. Appl. Pharm. 361, 62–67.
Musumeci, G., Loreto, C., Cardile, V., Carnazza, M.L., Martinez, G., 2010. Immunohistochemical expression of retinoblastoma and phospho-retinoblastoma protein in sheep lung exposed to fluoro-edenite fibers. Anat. Sci. Int. 85, 74–78.
Musumeci, G., Cardile, V., Fenga, C., Caggia, S., Loreto, C., 2011. Mineral fibre toxicity: expression of retinoblastoma (Rb) and phospho-retinoblastoma (pRb) protein in alveolar epithelial and mesothelial cell lines exposed to fluoro-edenite fibres. Cell Biol. Toxicol. 27, 217–225.
Naik, S.L., Lewin, M., Young, R., Dearwent, S.M., Lee, R., 2017. Mortality from asbestos-associated disease in Libby, Montana 1979–2011. J. Expo. Sci. Env. Epid. 27, 207–213.
NIOSH, 1994a. Asbestos and Other Fibers by Phase Contrast Microscopy (PCM), NIOSH Method 7400, Issue 2. National Institute for Occupational Safety and Health.
NIOSH, 1994b. Asbestos by Transmission Electron Microscopy (TEM), NIOSH Method 7402, Issue 2. National Institute for Occupational Safety and Health.
Pacella, A., Fantauzzi, M., Atzei, D., Cremisini, C., Nardi, E., Montereali, M.R., Rossi, A., Ballirano, P., 2017. Iron within the erionite cavity and its potential role in inducing its toxicity: evidence of Fe (III) segregation as extra-framework cation. Microporous Mesoporous Mater. 237, 168–179.
Pacella, A., Andreozzi, G.B., Nodari, L., Ballirano, P., 2019. Chemical and structural characterization of UICC crocidolite fibres from Koegas Mine, Northern Cape (South Africa). Period. Mineral. 88, 297–306.
Paoletti, L., Batisti, D., Bruno, C., Di Paola, M., Gianfagna, A., Mastrantonio, M., Nesti, M., Comba, P., 2000. Unusually high incidence of malignant pleural mesothelioma in a town of eastern Sicily: an epidemiological and environmental study. Arch. Environ. Health 55, 392–398.
Pollastri, S., Gualtieri, A.F., Lassinantti Gualtieri, M., Hanuskova, M., Cavallo, A., Gaudino, G., 2014. The zeta potential of mineral fibres. J. Hazard. Mater. 276, 469–479.
Pollastri, S., Perchiazzi, N., Gigli, L., Ferretti, P., Cavallo, A., Bursi Gandolfi, N., Pollok, K., Gualtieri, A.F., 2017a. The crystal structure of mineral fibres. 2. Amosite and fibrous anthophyllite. Period. Mineral. 86, 55–65.
Pollastri, S., Gigli, L., Ferretti, P., Andreozzi, G.B., Bursi Gandolfi, N., Pollok, K., Gualtieri, A.F., 2017b. The crystal structure of mineral fibres. 3. Actinolite asbestos. Period. Mineral. 86, 89–98.
Pozzolini, M., Vergani, L., Ragazzoni, M., Delpiano, L., Grasselli, E., Voci, A., Giovine, M., Scarfì, S., 2016. Different reactivity of primary fibroblasts and endothelial cells towards crystalline silica: a surface radical matter. Toxicol. 361, 12–23.
Pugnaloni, A., Giantomassi, F., Lucarini, G., Capella, S., Belmonte, M.M., Orciani, M., Belluso, E., 2010. Effects of asbestiform antigorite on human alveolar epithelial A549 cells: a morphological and immunohistochemical study. Acta Histochem. 112, 133–146.
Pugnaloni, A., Lucarini, G., Rubini, C., Smorlesi, A., Tomasetti, M., Strafella, E., Armeni, T., Gualtieri, A.F., 2015. Raw and thermally treated cement asbestos exerts different cytotoxicity effects on A549 cells *in vitro*. Acta Histochem. 117, 29–39.
Qi, F., Okimoto, G., Jube, S., Napolitano, A., Pass, H.I., Laczko, R., Demay, R.M., Khan, G., Tiirikainen, M., Rinaudo, C., Croce, A., Yang, H., Gaudino, G., Carbone, M., 2013. Continuous exposure to chrysotile asbestos can cause transformation of human mesothelial cells via HMGB1 and TNF-alpha signaling. Am. J. Pathol. 183, 1654–1666.
Roggli, V.L., 2015. The so-called short-fiber controversy: literature review and critical analysis. Arch. Pathol. Lab. Med. 139, 1052–1057.
Roggli, V.L., Green, C.L., 2019. Dimensions of elongated mineral particles: a study of more than 570 fibers from more than 90 cases with implications for pathogenicity and classification as asbestiform vs. Cleavage fragments. Ultrastruct. Pathol. 43, 1–5.
Schieber, M., Chandel, N.S., 2014. ROS function in redox signaling and oxidative stress. Curr. Biol. 24, R453–R462.
Schinwald, A., Murphy, F.A., Prina-Mello, A., Poland, C.A., Byrne, F., Movia, D., Glass, J. R., Dickerson, J.C., Schultz, D.A., Jeffree, C.E., MacNee, W., Donaldson, K., 2012. The threshold length for fiber-induced acute pleural inflammation: shedding light on the early events in asbestos-induced mesothelioma. Toxicol. Sci. 128, 461–470.
Stanton, M.F., Layard, M., Tegeris, A., Miller, E., May, M., Morgan, E., Smith, A., 1981. Relation of particle dimension to carcinogenicity in amphibole asbestoses and other fibrous minerals. J. Natl. Cancer Inst. 67, 965–975.
Thomas, D.C., 2017. The phagocyte respiratory burst: historical perspectives and recent advances. Immunol. Lett. 192, 88–96.
Travaglione, S., Bruni, B., Falzano, L., Paoletti, L., Fiorentini, C., 2003. Effects of the new-identified amphibole fluoro-edenite in lung epithelial cells. Toxicol. In Vitro 17, 547–552.
Travaglione, S., Bruni, B.M., Falzano, L., Filippini, P., Fabbri, A., Paoletti, L., Fiorentini, C., 2006. Multinucleation and pro-inflammatory cytokine release promoted by fibrous fluoro-edenite in lung epithelial A549 cells. Toxicol. In Vitro 20, 841–850.
Tsujimori, T., Matsumoto, K., Wakabayashi, J., Liou, J.G., 2006. Franciscan eclogite revisited: reevaluation of the P–t evolution of tectonic blocks from Tiburon Peninsula, California. USA. Miner. Petrol. 88, 243.
Wang, T.Y., Libardo, M.D.J., Angeles-Boza, A.M., Pellois, J.P., 2017. Membrane oxidation in cell delivery and cell killing applications. ACS Chem. Biol. 12, 1170–1182.
Wang, Y., Huo, T., Feng, C., Zeng, Y., Yang, J., Zhang, X., Dong, F., Deng, J., 2019. Chrysotile asbestos induces apoptosis via activation of the p53-regulated mitochondrial pathway mediated by ROS in A549 cells. Appl. Clay Sci. 182, 105245.
Xu, A., Zhou, H., Yu, D.Z., Hei, T.K., 2002. Mechanisms of the genotoxicity of crocidolite asbestos in mammalian cells: implication from mutation patterns induced by reactive oxygen species. Environ. Health. Persp. 110, 1003–1008.
Yang, H., Chao, L., Yang, D., Zhang, H., Xi, Z., 2009. Comparative study of cytotoxicity, oxidative stress and genotoxicity induced by four typical nanomaterials: the role of particle size, shape and composition. Comparative study of cytotoxicity, oxidative stress and genotoxicity. J. Appl. Toxicol. 29, 69–78.
Zoboli, A., Di Giuseppe, D., Baraldi, C., Gamberini, M.C., Malferrari, D., Urso, G., Lassinantti Gualtieri, M., Bailey, M., Gualtieri, A.F., 2019. Characterisation of fibrous ferrierite in the rhyolitic tuffs at Lovelock, Nevada, USA. Mineral. Mag. 83, 577–586.